



ELSEVIER

Journal of Nuclear Materials 266–269 (1999) 777–782

journal of  
nuclear  
materials

## Edge profiles and limiter tests in Extrap T2

H. Bergsåker \*, G. Hedin, L. Ilyinsky, D. Larsson, A. Möller

*Alfvén Laboratory, Royal Institute of Technology, (EURATOM/INFR Fusion Association) 100 44 Stockholm, Sweden*

### Abstract

New edge profile measurements, including calorimetric measurements of the parallel heat flux, were made in Extrap T2. Test limiters of pure molybdenum and the TZM molybdenum alloy have been exposed in the edge plasma. The surface damage was studied, mainly by microscopy. Tungsten coated graphite probes were also exposed, and the surfaces were studied by microscopy, ion beam analysis and XPS. In this case cracking and mixing of carbon and tungsten at the interface was observed in the most heated areas, whereas carbide formation at the surface was seen in less heated areas. In these tests pure Mo generally fared better than TZM, and thin and cleaner coatings fared better than thicker and less clean. © 1999 Elsevier Science B.V. All rights reserved.

*Keywords:* Reversed field pinch; High-z material; Surface damage

### 1. Introduction

The Extrap T2 reversed field pinch experiment has in its initial phase been operated with a complete graphite liner. This way there has been no danger of melting and other serious damage to the wall. By means of frequent helium glow discharge conditioning it has been possible to control the amount of hydrogen in the wall and hence to achieve stationary plasma densities in the range  $0.7\text{--}6 \times 10^{19} \text{ m}^{-3}$  [1,2].

However, the graphite wall also has a number of drawbacks. The long term memory effect with respect to hydrogen recycling makes it difficult to obtain shot to shot reproducibility. Low density operation requires a wall depleted of hydrogen [1,2]. But with little hydrogen in the wall there is always a large loss of particles in the start up phase of the discharge when confinement is poor. Unless the discharge is ignited at sufficiently high pressure this early pump out leads to disruption. However, a high filling pressure in turn entails a rapid buildup of trapped hydrogen and hence non stationary conditions.

More importantly, wall locked modes cause a localisation of the the heat flux to the wall, which is further enhanced due to poor alignment of the graphite tiles and

protruding edges. The pronounced thermal threshold effects in graphite, for enhanced chemical erosion and desorption from the rough and porous surface ( $T \approx 700 \text{ K}$ ) [3], for release of trapped hydrogen ( $T \approx 900 \text{ K}$ ) [4] and for radiation enhanced sublimation ( $T \approx 1400 \text{ K}$ ) [3] give rise to discrete events (rapid increase of density and/or impurity content) with deterioration of the plasma due to local thermal effects starting a few ms into the discharge.

In the second phase of operation which is under preparation, the vacuum vessel will be rebuilt for better diagnostic access and the graphite liner will be replaced with a set of molybdenum limiters. In order to investigate the effects of carbon specific plasma surface interactions before the graphite is removed, an experiment is being considered in which *ceteris paribus* the liner is coated with an in situ deposited thin tungsten layer.

In preparation for the metal wall experiments, the radial profiles of parallel heat flux were measured with calorimetric probes, and the data base on other edge profiles was extended. Test limiters made of molybdenum and the TZM (Ti, Zr, Mo) molybdenum alloy were exposed in the edge plasma. Graphite probes were coated with tungsten and exposed in a similar way. The surfaces were characterized before and after exposure with scanning electron microscopy (SEM), ion beam analysis methods (IBA) and X-ray photoelectron spectroscopy (XPS).

\* Corresponding author. Tel.: +46-8 101 033; fax: +46-8 158 674; e-mail: bergsaker@msi.se.

## 2. Experimental

The dimensions of Extrap T2 are major radius  $R = 1.24$  m and minor radius  $a = 0.183$  m. It has been operated with plasma current between 100 and 260 kA, and pulse lengths from 5 to 15 ms. The line average density has been in the range  $0.7\text{--}7 \times 10^{19} \text{ m}^{-3}$  and the central electron temperature from 100 to 200 eV, the energy confinement time 50–80  $\mu\text{s}$  [5].

Triple Langmuir probes and calorimetric probes of similar design as in [6] were inserted through a port on top of the machine. The same port was used when the molybdenum and TZM (Mo alloy by Plansee GmbH, with 0.5% Ti and 0.08% Zr) test limiters were inserted, as shown in Fig. 1. These were sintered, mushroom shaped pieces, manufactured by the Plansee company, with a spherical surface with radius of curvature 25 mm joining

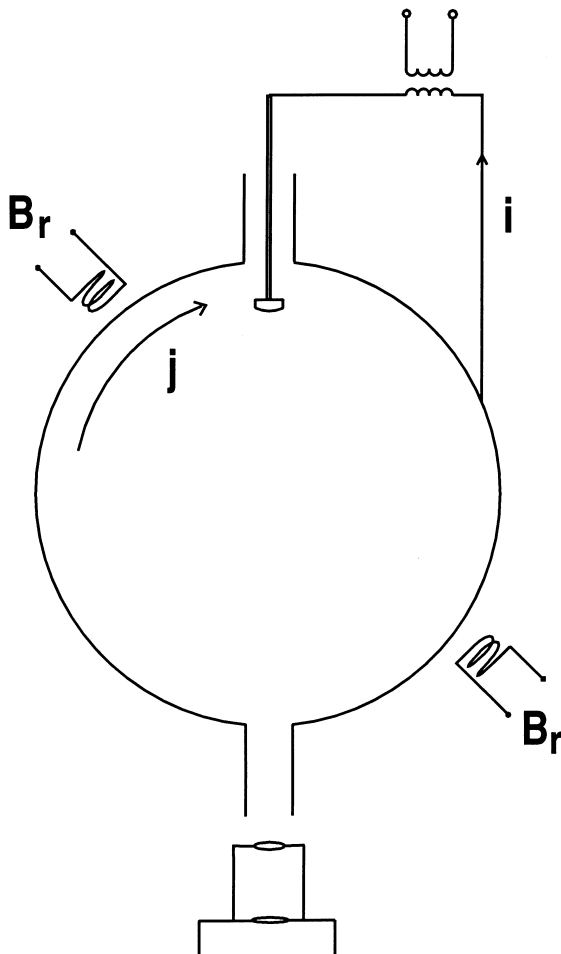


Fig. 1. Exposure of the test limiters through a vertical port. The limiters were viewed through the plasma, the current to the limiters was monitored and local plasma displacement was detected by picup coils.

smoothly a cylindrical surface with diameter 22 mm. The limiters were viewed through the plasma with a camera mounted on a window vertically below. Picup coils at two poloidal positions and at two adjacent toroidal positions were used to measure the radial or vertical field outside the vessel. The limiters were grounded to the vessel and the net current they were drawing was monitored. The same procedure was followed for both materials, the limiter was exposed to 18–20 discharges with 150 kA plasma current with the leading edge at  $r = 161$  mm and was taken out and investigated. It was then inserted to  $r = 153$  mm and again exposed to 20 discharges with  $I_p = 150$  kA, taken out and investigated.

Tungsten coatings were deposited on graphite cylinders with 10 mm diameter [1], using an in house designed planar magnetron system. The layer thicknesses were between 150 and 700 nm. Some of the depositions were made with poorer vacuum conditions ( $10^{-5}$  Torr base pressure rather than  $10^{-7}$  Torr) and in these cases the layers were found qualitatively by XPS to be more oxidized at the surface. Five of the coated cylinders were inserted vertically from another top port and exposed with the leading edge at  $r = 173$  mm to 2–8 discharges. After exposure they were removed using an UHV transport vessel [1] and moved to surface analysis stations for XPS and IBA investigation.

## 3. Results

Fig. 2 shows edge profiles of the electron temperature  $T_e$ , density  $n_e$ , floating potential  $V_f$  and parallel heat flux to a floating surface. The Langmuir probe data are an average over the time interval from 2 to 3 ms in 532 discharges. About 170 discharges were discarded because of mode locking close to the probe, which would make the interpretation difficult. The density was calculated from the ion saturation current density  $j_+$  using the relation  $j_+ = 0.5n_e\sqrt{2kT_e/m_i}$ . The temperature profiles are exponential with characteristic length  $\lambda_T$  in the range 9–15 mm, the steeper gradients occurring for the higher plasma currents. The density profiles are almost flat for  $r < 175$  mm but drop sharply close to the wall. The floating potential is reproducible, with a broad minimum around  $r = 165$  mm, and independent of current.

The heat flux data that are shown are an average over 80 complete discharges with 140–150 kA plasma current. In this case no correction was made for mode locking close to the probe and there is a shot to shot scatter of the data within a factor 3 which can probably be attributed to local displacements of the plasma current due to locked modes. The heat flux in 180 kA discharges was practically the same, both in slope and in level.

Inserting the test limiters to  $r = 161$  or 153 mm did not produce any significant effect on the global plasma parameters, but the data are consistent with an increase

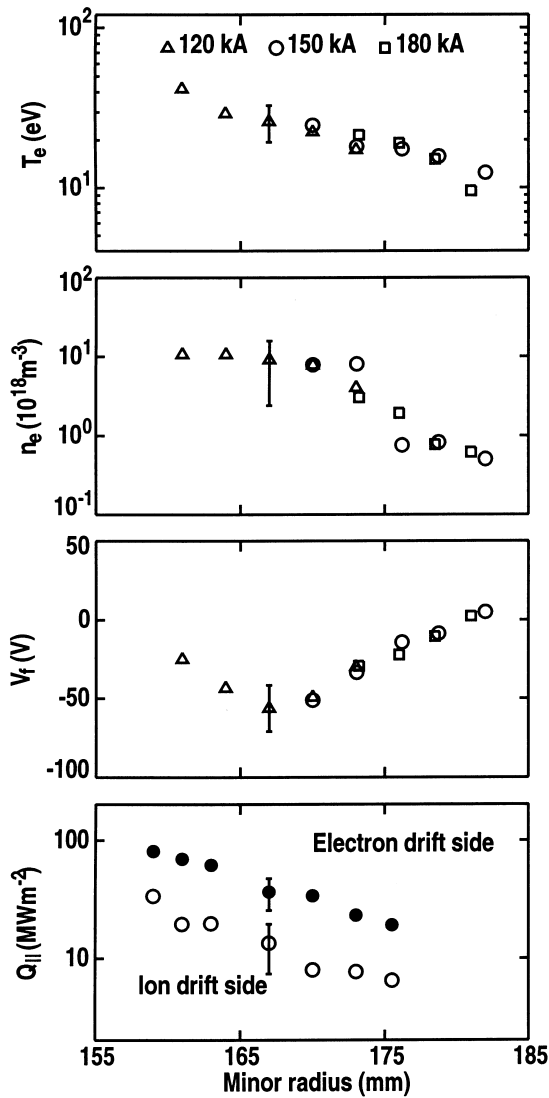
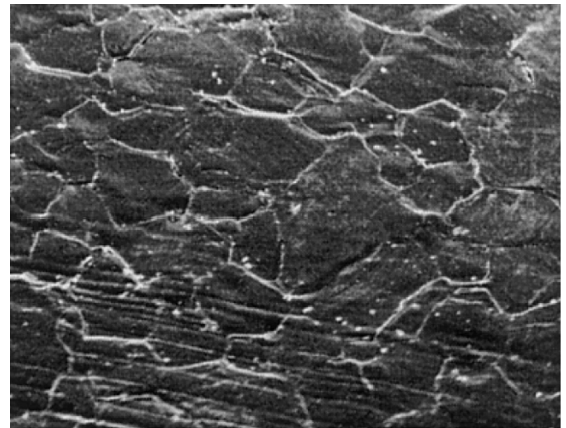


Fig. 2. Edge profiles of electron temperature, density and floating potential between 2 and 3 ms. Average parallel heat flux in 150 kA discharges.

in the loop voltage of 0–5 V or a reduction of the discharge duration by 0–1 ms for the deeper insertion.

Most of the time the test limiters were drawing negative current, typically from 100–400 A, which corresponds roughly to electron saturation current. Occasionally there were stationary phases with almost no current, or 10–20 A positive current, as expected for ion saturation, or fast spikes of up to 100 A positive current, suggesting arcs. During exposure there was consistently stronger light emission at the ion drift side edge of the limiters than on the opposite side. In about 20% of the discharges strong localized light emission was also observed, suggesting arcing.

The damage that was observed on the surfaces after exposure were melting, cracking and arc tracks. Recrystallization and melting was observed on the electron drift side at the corner where the surface became perpendicular to the magnetic field, both for the pure molybdenum limiter and the TZM limiter, particularly for the deeper insertion (corner at  $r=156$  mm). The molybdenum only showed microscopic cracks associated with the grain structure (Fig. 3(a)), whereas the TZM sample showed both microscopic and macroscopic cracks (Fig. 3(b)). Many types of arc tracks were observed: diffuse, fern like, single spots and lines. The



50 microns (a)



500 microns (b)

Fig. 3. Damage at the electron drift side corner on the test limiters. (a) Pure molybdenum, the cracks are only microscopic and related to the grain structure. (b) TZM, both microscopic and much larger cracks, parallel to the heat flux gradient are seen.

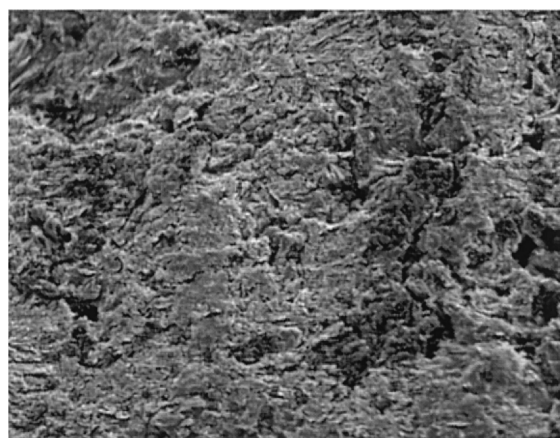
molybdenum sample collected up to  $10^{21}$  C/m<sup>2</sup> on the electron drift side of the spherical surface.

In the limited set of probes which were exposed, the damage to the tungsten coated graphite probes appeared to depend on the film thickness and on the oxidation state, cleaner thin layers performing better than thick and contaminated layers. Fig. 4 shows the surface after plasma exposure at a position 0.5 mm from the leading edge on the electron drift side ( $r=173$  mm). In Fig. 4(a) we see a 700 nm thick coating which had been produced at the higher base pressure. The sample was exposed to



50 microns

(a)

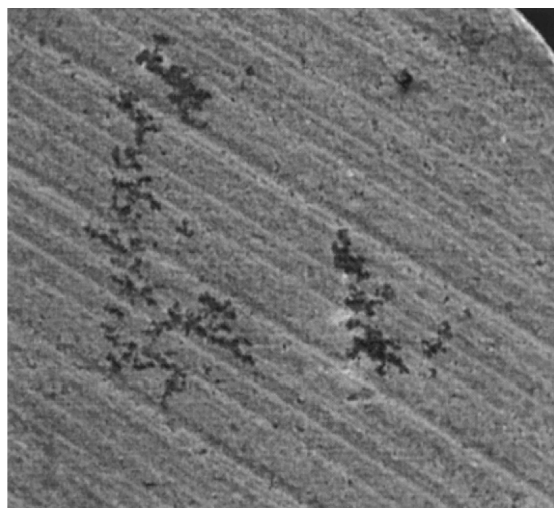


500 microns

(b)

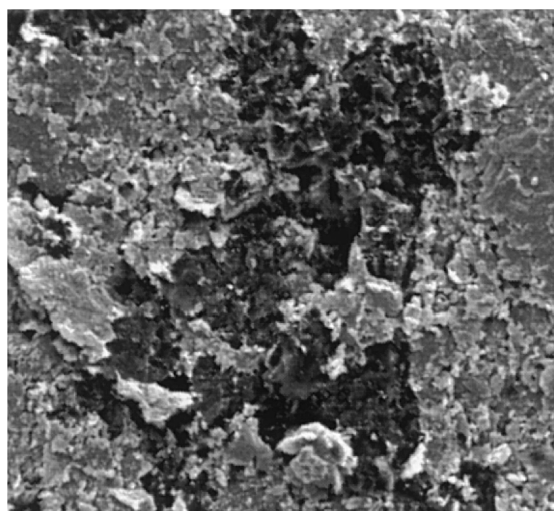
Fig. 4. Tungsten coated graphite surface near the electron drift side corner. (a) A 700 nm thick layer, oxidized before exposure. Exposed to four discharges at  $r=173$  mm. Severe cracking and flaking is observed. (b) A 150 nm thick, cleaner layer. Exposed to eight discharges at  $r=173$  mm. The layer is intact.

four discharges. The layer has cracked and partly flaked off. Fig. 4(b) shows the corresponding appearance of a probe with a 150 nm tungsten coating that had been prepared with the lower base pressure. In this case the sample has been exposed to eight discharges, but the coating is not as damaged as the thicker layer. Even in this case however, unipolar arcing can produce serious damage as shown in Fig. 5. The pictures show an arc track on the surface that was parallel to the wall (ex-



1 microns

(a)



20 microns

(b)

Fig. 5. Damage to a 150 nm tungsten coating due to unipolar arcs at a surface parallel to the wall,  $r=173$  mm, exposed to eight discharges.

posed to eight discharges at  $r = 173$  mm). The arc has caused the film to break and peel off.

Surface analysis showed cases of mixing of carbon and tungsten, not only near the hot corners of the samples, but also on the front surface that was exposed parallel to the wall. Fig. 6 shows such an example. The XPS spectra have been recorded before and after exposure to two discharges. After the exposure about 25% of the surface carbon is in the state of tungsten carbide [7]. In this case ion beam analysis by elastic proton back-scattering shows that the carbon depth profile is peaked at the surface, suggesting that the carbide formation is due to plasma deposited carbon. Near the hot corners mixing of carbon and tungsten at the interface can also be seen.

#### 4. Discussion

For the plasma currents 120–150 kA the average electron temperature profile in the region  $r < 175$  mm can be represented with  $T_e(r) = T_e(r_0) \exp(-r/\lambda_T)$ , with  $r_0 = 155$  mm,  $kT_e(r_0) = 60$  eV and  $\lambda_T = 15$  mm. Similarly  $n_e(r) = n_e(r_0) \exp(-r/\lambda_n)$  with  $n_e(r_0) = 1.9 \times 10^{19} \text{ m}^{-3}$  and  $\lambda_n = 25$  mm. The parallel heat flux in the ion- and electron drift directions are  $q_{i,e}(r) = q_{i,e}(r_0) \exp(-r/\lambda_{q,i,e})$ , with  $q_i(r_0) = 40 \text{ MW/m}^2$ ,  $q_e(r_0) = 120 \text{ MW/m}^2$  and  $\lambda_q = 11$  mm.

The asymmetric heat flux at the edge is a well established phenomenon in reversed field pinches. We interpret the total heat flux as being composed of a symmetric part and a contribution from superthermal electrons which move preferentially in the electron drift direction:  $q_{\text{tot}} = q_s + q_{\text{hot}}$ . Identifying  $q_i = q_s$  and  $q_e = q_s + q_{\text{hot}}$  we find that  $q_{\text{hot}} = 2q_s$ . Applying the standard theory [8] to the symmetric part we expect

$$q_s = \delta kT_e \frac{j_+}{e}, \quad (1)$$

where for a floating surface the sheath transmission factor

$$\delta = \frac{2T_i}{T_e} + \frac{2}{1 - \gamma_e} - 0.5 \ln \left[ \left( 2\pi \frac{m_e}{m_i} \right) \left( 1 + \frac{T_i}{T_e} \right) (1 - \gamma_e)^{-2} \right], \quad (2)$$

where  $\gamma_e$  is the secondary electron yield. For constant  $T_i/T_e$  we expect  $\lambda_q = \lambda_T \lambda_n / (\lambda_T + 1.5\lambda_n)$ , which is significantly smaller than the measured  $\lambda_q$ . From the measured profiles we can derive  $\delta$  as increasing from  $\delta = 6$  at  $r = 161$  mm to  $\delta = 10$  at  $r = 173$  mm, corresponding to  $T_i/T_e$  increasing from 1 to 3. This is not unreasonable if the ion temperature profiles are flatter than  $T_e$ .

When a grounded surface is inserted in a plasma with plasma potential  $V_p$  the sheath transmission factor becomes approximately [8]

$$\delta = \frac{eV_p}{kT_e} + \frac{2T_i}{T_e} + 2 e^{-eV_p/kT_e} \sqrt{\left( 1 + \frac{T_i}{T_e} \right) \left( \frac{2\pi m_e}{m_i} \right)}. \quad (3)$$

The plasma potential can be approximated with  $V_p = V_f + 2.5 kT_e/e$ . Using the (extrapolated) data from Fig. 2 yields a plasma potential of  $V_p \approx 140$  V at  $r = 156$  mm and  $V_p \approx 10$  V at  $r = 173$  mm, and a  $\delta$  of 5 and 15, respectively. Adding the same hot electron contribution as before we expect an average heat flux of  $110 \text{ MW/m}^2$  to the electron drift side corner of the deeply inserted limiters. With thermal data for molybdenum this corresponds to a temperature rise at the surface of  $600^\circ\text{C}$  in a 10 ms discharge. Similarly the expected temperature rise at the hot edge of the graphite probes would be  $250^\circ$ . However, the large negative currents to the limiters suggest that the plasma potential may have been lower and the heat flux higher, as required to produce melting.

The pure molybdenum limiter performed better than the TZM, which may be due either to the poorer heat conductivity or to preexisting stress in the sample. The cleaner 150 nm coating did not crack significantly and may be possible for liner coating. However there is likely to be significant damage due to unipolar arcs. The carbide formation on the tungsten coated samples is another important finding, particularly where it occurred due to carbon deposition on surfaces that were not excessively heated. A carbide surface layer would change the hydrogen recycling properties from metal like to

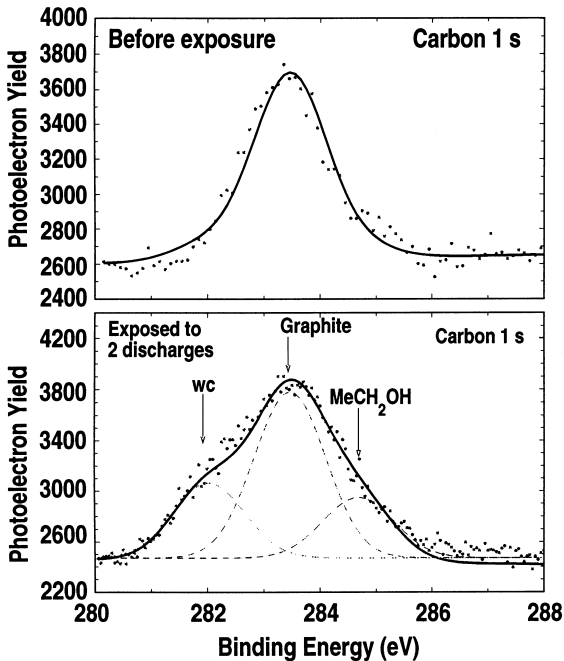


Fig. 6. X-ray photoelectron spectra from a tungsten coated surface parallel to the wall. Tungsten carbide is formed at the surface after exposure to two discharges at  $r = 173$  mm.

more carbon like, e.g. with large hydrogen trapping at room temperature [9,10]. On edges and other small areas this would not be important, since the particle flux to the wall is much more uniformly distributed than the heat flux, but if it covers larger areas it has to be taken into account.

Magnetic pickup measurements indicate that the plasma column is displaced by typically 15 mm or so in the area where modelocking to the wall occurs. If the heat flux on the flux surfaces is conserved and with  $\lambda_q = 11$  mm this corresponds to an increase by a factor of four in the heat flux to protruding edges at the wall. This number fits reasonable well with the shot to shot scatter in the heat flux at a fixed position, if the modes lock at random positions. However no clear correlation was seen between the heat flux to the probe and the toroidal position of the wall locked modes. It is expected that improved viewing of the inner wall will clarify the interpretation.

## 5. Conclusions

Edge profiles of parallel heat flux, electron temperature, density and floating potential were measured in T2. The profiles are consistent with a symmetric contribution to the heat flux due to maxwellian electrons and ions with  $T_e \leq T_i \leq 3T_e$  plus a hot electron contribution that is twice higher. Test limiters of molybdenum and TZM and tungsten coated graphite probes were exposed in the edge plasma and the damage to the surfaces was

investigated. Tungsten layers which were not thicker than 150 nm and sufficiently clean did not crack or flake off. Serious damage due to arcing did occur. Tungsten carbide formation with plasma deposited carbon was observed, as well as mixing of carbon and tungsten in the most heated areas.

## References

- [1] H. Bergs aker, D. Larsson, P. Brunsell et al., *J. Nucl. Mater.* 241–243 (1997) 993.
- [2] D. Larsson, H. Bergs aker, *Proc. 24th Eur. Conf. Contr. Fusion and Plasma Phys. Berchtesgaden 1997, Part III*, p. 1233.
- [3] J. Roth, E. Vietzke, A.A. Haasz, *Nucl. Fus. Suppl. Atom. Plasm. Mater. Interact. Dat. Fus.* 1 (1991) 63.
- [4] W. M oller, *J. Nucl. Mater.* 162–164 (1989) 138.
- [5] J.R. Drake, H. Bergs aker, P.R. Brunsell et al., *Fusion Energy 1996, Montreal, Canada, IAEA, Vienna, 1997*, vol. 2, p. 193.
- [6] H. Bergs aker, A. M oller, G.X. Li et al., *J. Nucl. Mater.* 220–222 (1995) 712.
- [7] C.D. Wagner et al., G.E. Muilenberg, *Handbook of X-ray Photoelectron Spectroscopy*, Perkin–Elmer.
- [8] P. Stangeby, in: D.E Post, R. Behrisch (Eds.), *Physics of Plasma–wall Interactions in Controlled Fusion Devices*, Plenum, New York, 1986.
- [9] P. Franzen, C. Garcia-Rosales, H. Plank et al., *J. Nucl. Mater.* 241–243 (1997) 1082.
- [10] W. Wang, V. Kh. Alimov, B.M.U. Scherzer et al., *J. Nucl. Mater.* 241–243 (1997) 1087.